

Iterative Synchronization for Dually-Polarized Independent Transmission Streams

Marco Martalò, *Senior Member, IEEE*, Gianluigi Ferrari, *Senior Member, IEEE*,
Muhammad Asim, *Student Member, IEEE*, Jonathan Gambini, Christian Mazzucco,
Giacomo Cannalire, Sergio Bianchi, and Riccardo Raheli, *Member, IEEE*

Abstract—In this paper, we investigate a wireless communication scenario, where polarization multiplexing is exploited to increase the spectral efficiency. Independent modems over each polarization are considered, with communication links affected by phase noise and cross-polarization interference (XPI). We devise a novel per-polarization soft decision-directed iterative receiver with separate *a posteriori* probability-based synchronization and decoding. The synchronization algorithm relies on a minimum mean square error-based master-slave phase estimation followed by the cancellation of the XPI on the polarization of interest and requires no statistical knowledge of the phase noise process. The performance of the proposed iterative receiver is investigated for a pilot symbol-assisted low-density parity-check-coded quadrature amplitude modulation scheme.

Index Terms—Dually-polarized radio communication, phase noise suppression, iterative decoding, synchronization, minimum mean square error (MMSE).

I. INTRODUCTION

MODERN wireless communication systems must support a rapidly increasing information rate and spectral efficiency. A well-known method to increase the data rate is represented by antenna polarization multiplexing, i.e., two data streams are transmitted at the same carrier frequency by ideally orthogonal polarizations, such as vertical and horizontal [1]. Since, in practice, the two polarizations are not perfectly orthogonal, there may be some energy leakage between them, thus generating the so-called Cross-Polarization Interference (XPI). This imperfection may be counter-acted

by designing proper Cross-Polarization Interference Cancellation (XPIC) algorithms at the receiver [1]. Although dual polarization communication is well established, it is still of significant interest as a potential technology to improve the spectral efficiency of existing microwave backhaul radio links [2]–[4]. In the remainder of this manuscript, we refer to such schemes as Dual-Polarization (DP) systems.

DP systems and XPIC design are well-established topics in both the fields of wireless [1] and coherent fiber optic communications [5]–[7]. More generally, synchronous streams can be transmitted on multiple channel modes, so that combined signal detection can be exploited by accounting for useful and interfering signals as in Multiple Input Multiple Output (MIMO) communications [8], [9]. Unlike these systems, this paper focuses on DP systems with independent transmission streams. More specifically, the design of flexible and cost-efficient solutions based on two separate outdoor microwave units, one per polarization, with independent radio frequency local oscillators, asynchronous sampling, and analog signal exchange between polarizations at intermediate frequency only is of interest. In this case, a joint decoding approach, where the receiver can have direct access to phase estimates and data decisions of both polarizations and exploit them for XPIC, cannot be pursued. Since the majority of the overall deployed systems use a single polarization, the approach proposed here allows maximum flexibility in interconnecting and gradually replacing single polarization modules with DP modems within the same network: this can be a strategic technological approach to support the ambitious backhaul requirements in 5G systems [10].

In this context, our goal is to design a phase recovery algorithm for DP systems in which independent modems are employed over the two polarizations. In particular, we propose a novel iterative receiver, where demodulation and decoding are performed separately from phase estimation. These operations may rely on “off-the-shelf” demapper and soft-output decoder, in which phase estimation is based on a Master-Slave (MS) [11] Minimum Mean Square Error (MMSE)-based algorithm and exploits the symbol *A Posteriori* Probabilities (APPs) generated by the demapper/decoder. Our approach allows to implement pragmatic synchronization schemes. However, unlike our previous contribution for single polarization schemes [12], here we resort to a novel solution in order to account for the peculiarity of DP systems with independent streams employing XPIC. To the best of our knowledge,

Manuscript received October 13, 2016; revised February 14, 2017; accepted March 20, 2017. Date of publication March 28, 2017; date of current version June 14, 2017. This paper was presented at the IEEE International Symposium on Wireless Communication Systems, Brussels, Belgium, 2015. The associate editor coordinating the review of this paper and approving it for publication was G. M. Vitetta. (*Corresponding author: Marco Martalò.*)

M. Martalò is with the Department of Engineering and Architecture, University of Parma, Parma, Italy, and also with E-Campus University, Novedrate, Italy (e-mail: marco.martalò@unipr.it).

G. Ferrari and R. Raheli are with the Department of Engineering and Architecture, University of Parma, Parma, Italy (e-mail: gianluigi.ferrari@unipr.it; riccardo.raheli@unipr.it).

M. Asim was with the University of Parma, Italy. He is now with the Department of Computer Science, Preston University, Peshawar, Pakistan (e-mail: muhammad.asim@unipr.it).

J. Gambini, C. Mazzucco, G. Cannalire, and S. Bianchi are with the European Research Center, Huawei Technologies, Milan, Italy (e-mail: jonathan.gambini@huawei.com; christian.mazzucco@huawei.com; giacomo.cannalire@huawei.com; sergio.bianchi@huawei.com).

Color versions of one or more of the figures in this paper are available online at <http://ieeexplore.ieee.org>.

Digital Object Identifier 10.1109/TCOMM.2017.2688398

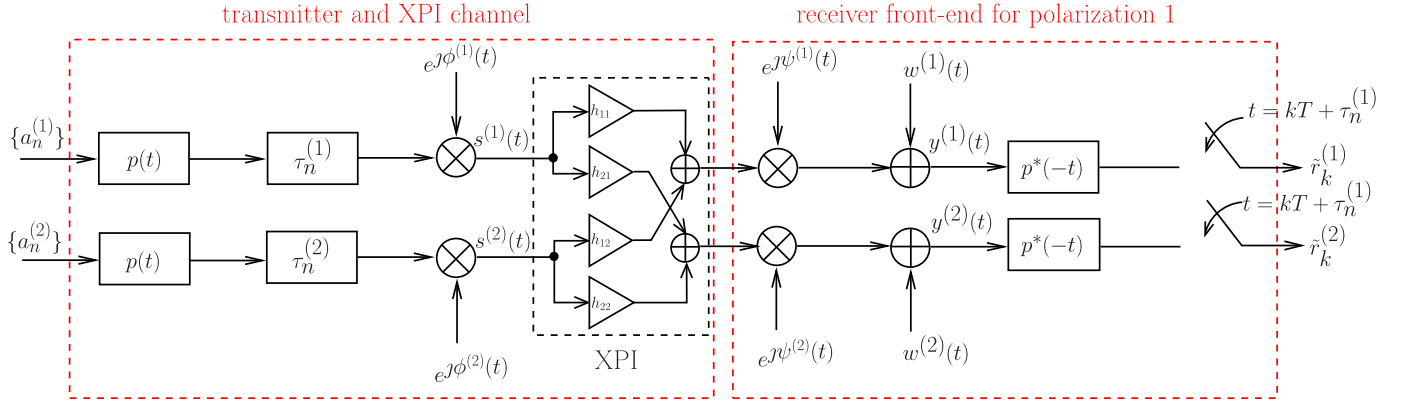


Fig. 1. Continuous-time system model.

our paper is the first in the literature proposing an iterative receiver for such a problem. Preliminary results on this subject presented in [13] are here extended and consolidated in terms of a generalized phase synchronization algorithm with a proper filtering strategy and comprehensive numerical results. As a representative case study, we perform a simulation-based analysis for Low Density Parity Check (LDPC)-coded Quadrature Amplitude Modulation (QAM) systems with pilot symbols. Our results show good performance for medium-high constellation sizes and large phase noise intensities.

The paper is organized as follows. In Section II, the reference system model is described. In Section III, the MMSE-based phase estimation algorithm is derived. The iterative demapping/decoding and synchronization receiver for DP systems is presented in Section IV and its performance is investigated in Section V. Finally, conclusions are drawn in Section VI.

II. SYSTEM MODEL

Consider the DP system model with XPI, phase noise, and Additive White Gaussian Noise (AWGN) depicted in Fig 1. The indexes 1 and 2 refer to co-polar (i.e., useful) and cross-polar (i.e., interfering) signals, respectively. Let us denote as $a_n^{(i)}$ the n -th coded modulated symbol on the i -th polarization, $i = 1, 2$. These symbols are obtained by encoding an information sequence using a binary channel code, with code rate R , and mapping it onto a sequence of modulated symbols, whose generic element $a_n^{(i)}$ belongs to a constellation of size $M = 2^b$ and average symbol energy E_s . The coded modulation scheme is assumed identical on both polarizations to keep the notation simple. However, the proposed approach is valid for different codes and modulations on the two polarizations.¹ The multi-level coding scheme described in [12] is considered to enable spectrally efficient modulations and keep the coding strategy unaltered even if the modulation order increases. In particular, for small constellation sizes all bits are channel encoded, whereas for medium/high-size constellations a multi-level coding approach in which b_1 out of b bits are encoded (“coded” bits) and the remaining $b_2 = b - b_1$ bits are

left uncoded (“free” bits) is adopted. According to Ungerboeck set partitioning, the coded bits identify one of 2^{b_1} possible subsets of a constellation with a total of 2^b points, whereas b_2 free bits specify a given point of the selected subset. In Section V, we shall focus on a representative case study with LDPC-coded M -QAM with $b_1 = 4$ and $M \geq 16$ in all the considered cases.

The modulated (continuous-time) signal on the i -th polarization can be written as

$$s^{(i)}(t) = \left[\sum_n a_n^{(i)} p(t - nT - \tau_n^{(i)}) \right] e^{j\phi^{(i)}(t)}$$

where T is the symbol interval, $p(t)$ is a pulse shaping response with square-root raised cosine transform, $\phi^{(i)}(t)$ represents the phase noise generated by the oscillators at the i -th transmitter, and $\tau_n^{(i)}$ is a proper slowly time-varying delay expedient to model asynchronous streams.

The receiver front-end for polarization 1, shown in the right-hand side of Fig. 1, first performs frequency downconversion, so that the baseband received signal is

$$\begin{aligned} y^{(i)}(t) &= \sum_{j=1}^2 h_{ij} s^{(j)}(t) e^{j\psi^{(i)}(t)} + w^{(i)}(t) \\ &= \sum_{j=1}^2 h_{ij} \left[\sum_n a_n^{(j)} p(t - nT - \tau_n^{(j)}) e^{j\phi^{(j)}(t)} \right] e^{j\psi^{(i)}(t)} \\ &\quad + w^{(i)}(t) \\ &= \sum_{j=1}^2 h_{ij} \sum_n a_n^{(j)} p(t - nT - \tau_n^{(j)}) e^{j[\psi^{(i)}(t) + \phi^{(j)}(t)]} \\ &\quad + w^{(i)}(t) \end{aligned}$$

where $w^{(i)}(t)$ is AWGN, $\psi^{(i)}(t)$ represents the phase noise generated by the oscillators at the i -th polarization demodulator, and h_{ij} is the element of the XPI matrix \mathbf{H} equal to

$$h_{ij} = \frac{1 + (\chi - 1)|i - j|}{\sqrt{1 + \chi^2}} \quad i, j = 1, 2$$

in which χ is a proper parameter which describes the cross-polarization interference intensity and the factor $1/\sqrt{1 + \chi^2}$ is introduced to normalize the rows and columns of \mathbf{H} to

¹Since the streams are independent, the receiver performance is not affected by the format of the cross-polarization signal treated as unknown interference.

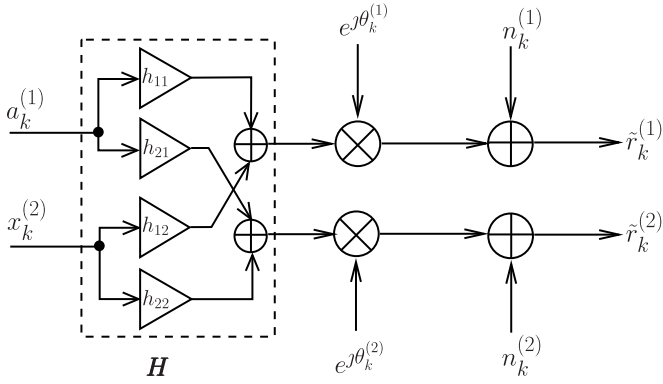


Fig. 2. Equivalent discrete-time system model for the receiver of polarization 1.

unitary norm. In the application of interest, the interfering cross-polar signal is assumed to have smaller intensity than the useful co-polar signal. This means that $|h_{ii}| > |h_{ij}|$ ($j \neq i$) and, therefore, $\chi < 1$.

Matched filtering and sampling synchronously with the co-polar branch (i.e., compensating for $\tau_n^{(1)}$) leads to

$$\tilde{r}_k^{(i)} = \sum_{j=1}^2 h_{ij} \sum_n a_n^{(j)} g((k-n)T - \tau_n^{(j)} + \tau_n^{(1)}) e^{j(\psi_k^{(i)} + \phi_k^{(j)})} + w_k^{(i)}$$

where $g(t) = p(t) \otimes p^*(-t)$ is a Nyquist pulse, $w_k^{(i)}$ are independent and identically distributed (i.i.d.) noise samples, and sufficiently slow phase variations are assumed. The terms $\psi_k^{(i)}$ and $\phi_k^{(i)}$, $i = 1, 2$, represent the sampled sequences at instant kT of the continuous-time processes $\psi^{(i)}(t)$ and $\phi^{(i)}(t)$, respectively. In other words, the co-polar received observable can be written as

$$\tilde{r}_k^{(1)} = h_{11}a_k^{(1)}e^{j\theta_k^{(1)}} + h_{12}x_k^{(2)}e^{j\theta_k^{(1)}} + w_k^{(1)} \quad (1)$$

where $\theta_k^{(1)} \triangleq \psi_k^{(1)} + \phi_k^{(1)}$ and

$$x_k^{(2)} \triangleq e^{j(\phi_k^{(2)} - \phi_k^{(1)})} \sum_n a_n^{(2)} g((k-n)T + \tau_n^{(1)} - \tau_n^{(2)}).$$

Using a similar derivation for the cross-polar received observable on the co-polar time base, one obtains

$$\tilde{r}_k^{(2)} = h_{21}a_k^{(1)}e^{j\theta_k^{(2)}} + h_{22}x_k^{(2)}e^{j\theta_k^{(2)}} + w_k^{(2)} \quad (2)$$

where $\theta_k^{(2)} \triangleq \psi_k^{(2)} + \phi_k^{(1)}$.

The equivalent discrete-time system model for the receiver of polarization 1 corresponding to (1) and (2) is shown in Fig. 2. Note that the model is fully characterized in terms of two phase noise processes only. The interfering signal $x_k^{(2)}$ accounts for all the effects caused by asynchronous phasing and timing on the cross polar signal. The discrete-time phase noise processes in (1) and (2) may be modeled by the well-established Wiener process with quadratic power spectrum decay [14], [15]:

$$\theta_k^{(i)} = \theta_{k-1}^{(i)} + \Delta_k^{(i)} \quad i = 1, 2$$

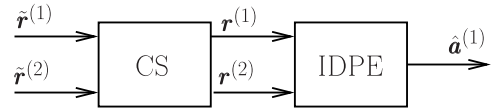


Fig. 3. Principle of the proposed two-stage receiver.

where $\Delta_k^{(i)} \sim \mathcal{N}(0, \sigma_\Delta^2)$ are i.i.d. Gaussian increments with zero mean and variance σ_Δ^2 , which is assumed equal for both polarizations and specifies the phase noise intensity. The use of other phase noise models can be easily accounted for, since the proposed receiver does not require any a priori statistical knowledge of the phase noise process. Besides compact and elegant, the equivalent model in Fig. 2 may be useful for simulations.

In the transmitted frame, pilot symbols [16] with energy E_p are inserted to enable initial synchronization when APPs are not available.² We assume that N_p pilot symbols are interleaved every N data symbols. The average bit Signal-to-Noise Ratio (SNR) is denoted as γ_b and takes into account the energy penalty due to pilot symbol insertion.

III. MMSE-BASED PHASE SYNCHRONIZATION

The considered receiver is sketched in Fig. 3 and composed of two stages. The vectors $\tilde{\mathbf{r}}^{(i)}$, $i = 1, 2$, containing a block of samples from the received signals on the two polarizations, feed the input of a Coarse Synchronization (CS) bootstrap stage. The goal of this stage is to coarsely reduce the phase noise affecting the received signals. The vectors output by the CS are denoted as $\mathbf{r}^{(i)}$, $i = 1, 2$, and are used to activate the iterative synchronization/detection procedure carried out by a subsequent Iterative Detection and Phase Estimation (IDPE) stage. The details on this stage will be presented in Section IV. Note also that we assume that the XPI channel matrix is known, since it can be estimated using “classical” algorithms. Moreover, time synchronization on the co-polar signal can be managed, for example, by a proper equalization stage at the receiver front-end. However, these investigations go beyond the scope of this paper. For the following discussion it suffices to assume that $\mathbf{r}^{(i)}$ is affected by XPI and phase noise according to the model (1)-(2) and suitably scaled to compensate for the channel coefficients.

The goal of this section, instead, is to derive the novel MMSE-based phase estimation algorithm embedded in the IDPE stage, which is an extension of the work in [12] to DP schemes. In particular, we assume constant phase noise over a (sufficiently short) observation window of ℓ consecutive samples, where ℓ is a proper system parameter to be optimized. This assumption is expedient to keep the computational complexity low, yet enabling accurate tracking of the phase noise. In Subsection III-A, we focus on disjoint consecutive windows. In Subsection III-B, we present an extension of this strategy to the use of a sliding window.

²Boosted pilot symbols, i.e., $E_p > E_s$, will be considered in the numerical results.

A. BW-Phase Estimation Algorithm

The MMSE-based phase estimation strategy is reminiscent of the MS phase synchronized first-order Phase-Locked Loop (PLL) as, e.g., discussed in [11]. The operational principle of MS Phase Estimation (PE) is to improve the phase tracking performance on both polarization branches: more precisely, a master PE algorithm corrects the phase noise affecting the co-polar signal, and a slave PE algorithm tracks the phase of the interferer.

The Block Window (BW) PE algorithm can be formalized as follows. We denote the ℓ -symbol block of observables (at the input of the IDPE) on the i -th ($i = 1, 2$) polarization branch starting at epoch k by the following row vector

$$\mathbf{r}_k^{(i)} \triangleq [r_k^{(i)}, r_{k+1}^{(i)}, \dots, r_{k+\ell-1}^{(i)}].$$

Similarly, we denote the block of corresponding transmitted symbols and estimated phases, respectively, as

$$\begin{aligned} \mathbf{a}_k^{(i)} &\triangleq [a_k^{(i)}, a_{k+1}^{(i)}, \dots, a_{k+\ell-1}^{(i)}] \\ \hat{\boldsymbol{\phi}}_k^{(i)} &\triangleq [\hat{\phi}_k^{(i)}, \hat{\phi}_{k+1}^{(i)}, \dots, \hat{\phi}_{k+\ell-1}^{(i)}]. \end{aligned}$$

As previously mentioned, the estimated phase processes over the ℓ symbols of the block starting at epoch k are kept constant, i.e.:

$$\hat{\boldsymbol{\phi}}_k^{(i)} = \hat{\phi}_k^{(i)} \mathbf{1}_\ell \quad i = 1, 2$$

where $\hat{\phi}_k^{(i)}$ is a scalar and $\mathbf{1}_\ell$ denotes the length- ℓ vector with all elements equal to 1. The k -th values for both polarizations will be collected in the two-element vector $\hat{\boldsymbol{\phi}}_k \triangleq [\hat{\phi}_k^{(1)}, \hat{\phi}_k^{(2)}]$. The overall phase estimate vector over the symbols associated with a particular codeword is denoted as $\hat{\boldsymbol{\phi}}^{(i)} \triangleq [\hat{\phi}_0^{(i)}, \dots, \hat{\phi}_{n_p-1}^{(i)}]$, where n_p is the number of disjoint blocks in a codeword.

Given the above model and temporarily assuming perfect knowledge of the co-polar data symbols $\mathbf{a}_{m\ell}^{(1)}$ (this assumption will be dropped later), the proposed BW estimation strategy within the m -th disjoint block is the solution of the following vectorial MMSE problem:

$$\hat{\boldsymbol{\phi}}_{m\ell} = \underset{\boldsymbol{\phi}_{m\ell}}{\operatorname{argmin}} \left\| \tilde{\mathbf{z}}_{m\ell}^{(1)} - \mathbf{a}_{m\ell}^{(1)} \right\|^2 \quad (3)$$

where $\|\cdot\|$ represents the Euclidean norm, $\boldsymbol{\phi}_{m\ell} = [\phi_{m\ell}^{(1)}, \phi_{m\ell}^{(2)}]$ is a trial vector, and

$$\tilde{\mathbf{z}}_{m\ell}^{(1)} \triangleq \left[\mathbf{r}_{m\ell}^{(1)} + \mathbf{r}_{m\ell}^{(2)} e^{-j\phi_{m\ell}^{(2)}} \right] e^{-j\phi_{m\ell}^{(1)}}. \quad (4)$$

The rationale behind (3) is the use of the modified observable $\tilde{\mathbf{z}}_{m\ell}^{(1)}$, as defined in (4), which is obtained from the properly scaled observable on the co-polar branch $\mathbf{r}_{m\ell}^{(1)}$ by first eliminating the XPI (as done between square brackets) and, then, de-rotating this “cleaner” observable. If the correct phase rotations are used in (4), $\tilde{\mathbf{z}}_{m\ell}^{(1)} \simeq \mathbf{a}_{m\ell}^{(1)}$ but for the AWGN.

Using (4) into (3) and dropping irrelevant terms, straightforward manipulations lead to the following maximization problem:

$$\hat{\boldsymbol{\phi}}_{m\ell} = \underset{\boldsymbol{\phi}_{m\ell}}{\operatorname{argmax}} \Re \left\{ B e^{-j\phi_{m\ell}^{(1)}} + C e^{-j(\phi_{m\ell}^{(1)} + \phi_{m\ell}^{(2)})} + D e^{-j\phi_{m\ell}^{(2)}} \right\} \quad (5)$$

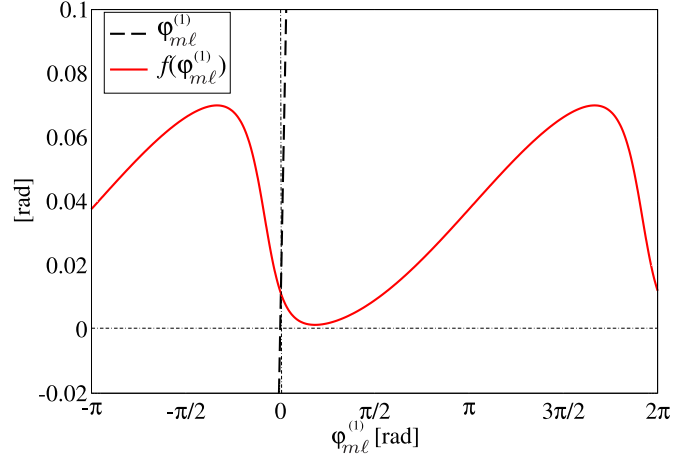


Fig. 4. Example realization of $f(\varphi_{m\ell}^{(1)})$ (as defined in (11)) in radians, for 64-QAM, $\gamma_b = 12.5$ dB and $\ell = 16$.

where

$$B \triangleq \mathbf{r}_{m\ell}^{(1)} \left(\mathbf{a}_{m\ell}^{(1)} \right)^\dagger \quad (6)$$

$$C \triangleq \mathbf{r}_{m\ell}^{(2)} \left(\mathbf{a}_{m\ell}^{(1)} \right)^\dagger \quad (7)$$

$$D \triangleq -\mathbf{r}_{m\ell}^{(2)} \left(\mathbf{r}_{m\ell}^{(1)} \right)^\dagger \quad (8)$$

in which \dagger is the Hermitian operator. We remark that the products in (6)-(8) are inner products and, therefore, B , C , and D are scalar complex quantities. From (5), given the trial value $\varphi_{m\ell}^{(2)}$, it follows that

$$\hat{\varphi}_{m\ell}^{(1)} = \arg \left[B + C e^{-j\varphi_{m\ell}^{(2)}} \right]. \quad (9)$$

Similarly, from (5), given the trial value $\varphi_{m\ell}^{(1)}$, one has

$$\hat{\varphi}_{m\ell}^{(2)} = \arg \left[D + C e^{-j\varphi_{m\ell}^{(1)}} \right]. \quad (10)$$

Inserting (10) into (9), one obtains the following fixed-point equation in the variable $\varphi_{m\ell}^{(1)}$

$$\hat{\varphi}_{m\ell}^{(1)} = \arg \left[B + C e^{-j \arg \left[D + C e^{-j\hat{\varphi}_{m\ell}^{(1)}} \right]} \right]. \quad (11)$$

The phase estimate $\hat{\varphi}_{m\ell}^{(2)}$ is consequently obtained as

$$\hat{\varphi}_{m\ell}^{(2)} = \arg \left[D + C e^{-j\hat{\varphi}_{m\ell}^{(1)}} \right]. \quad (12)$$

The solution of the fixed-point equation (11), of type $\varphi_{m\ell}^{(1)} = f(\varphi_{m\ell}^{(1)})$, can be obtained by leveraging any suitable numerical algorithm. In Fig. 4, an illustrative realization of $f(\varphi_{m\ell}^{(1)})$ is shown in radians, for 64-QAM modulation, $\gamma_b = 12.5$ dB and $\ell = 16$. One can observe that $f(\varphi_{m\ell}^{(1)})$ is a periodic function of $\varphi_{m\ell}^{(1)}$ and a unique intersection with the line $\varphi_{m\ell}^{(1)}$ exists. Therefore, the function $f(\varphi_{m\ell}^{(1)}) - \varphi_{m\ell}^{(1)}$ has only one zero, which corresponds to the unique solution of (11).

Although the uniqueness of the solution of this fixed-point equation cannot be analytically proved, in Fig. 5 a geometric interpretation of the optimization problem in (5)

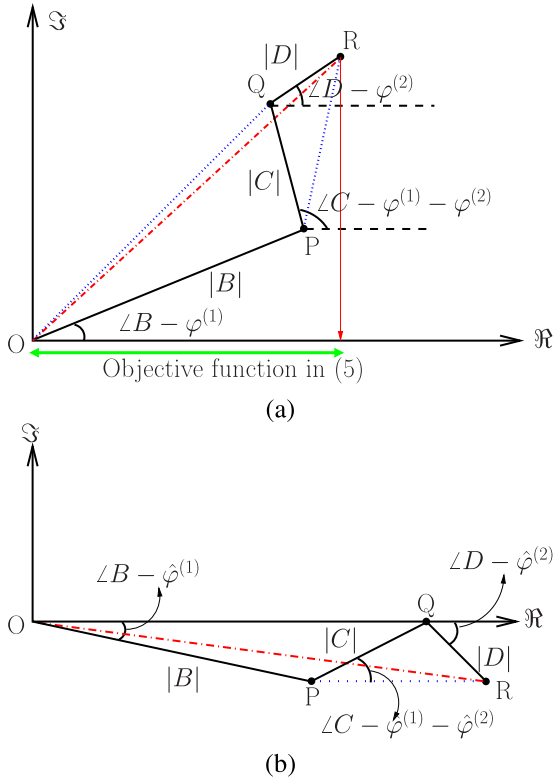


Fig. 5. Geometric interpretation of the optimization problem in (5): (a) general geometric setting and (b) optimal MMSE solution.

is shown, where, for simplicity, the block index m is dropped. In particular, in Fig. 5 (a) the general geometric setting is shown, with a representative indication of the three complex quantities which correspond to the three addenda inside the real part operator on the right-hand side of (5). The maximization problem in (5) is equivalent to selecting the two angles $\varphi^{(1)}$ and $\varphi^{(2)}$ so that the real part of the vector \mathbf{OR} is maximized. It can be geometrically shown, as illustrated in Fig. 5 (b), that the real part of the vector \mathbf{OR} is maximum when the vectors \mathbf{OQ} and \mathbf{PR} are parallel to the real axis (in particular, the vector \mathbf{OQ} lies on the real axis). This solution can be geometrically justified through the following iterative procedure.

- First, by varying the angle $\varphi^{(1)}$, it is possible to bring the point Q on the real axis: this is the “best” strategy to maximize the real part of the segment \mathbf{OR} by acting only on $\varphi^{(1)}$ for a given $\varphi^{(2)}$.
- At this point, by varying the angle $\varphi^{(2)}$ for a given $\varphi^{(1)}$, the real part of the segment \mathbf{OR} is maximized when the segment \mathbf{PR} is parallel to the real axis.
- The second step of the geometric optimization procedure might have moved the point Q off the real axis: if so, the angle $\varphi^{(1)}$ can be readjusted in order to bring Q on the real axis and to further maximize the real part of the segment \mathbf{OR} .
- Then, $\varphi^{(2)}$ and $\varphi^{(1)}$ can be recursively adjusted in order to reach the configuration in Fig. 5 (b). The corresponding final phases $\hat{\varphi}^{(1)}$ and $\hat{\varphi}^{(2)}$ are obtained according to the proposed MMSE strategy as in (11) and (12).

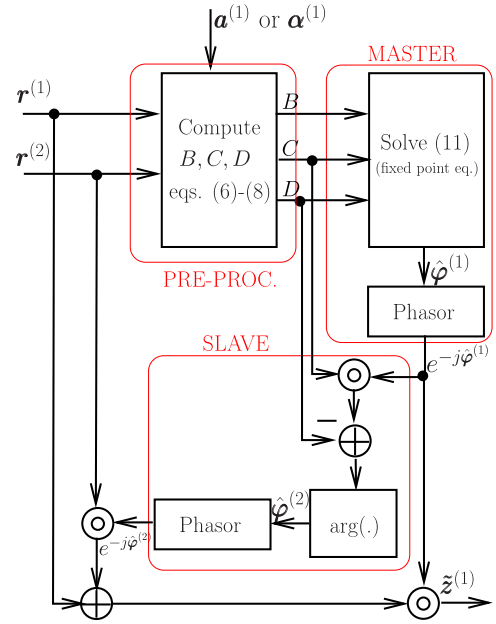


Fig. 6. Principle of the MS synchronization scheme, i.e., equations (11) and (12) for the polarization of interest.

In Fig. 6, the block diagram of the MS PE scheme corresponding to (11) and (12) is shown—the symbol \circ represents element-wise product between vectors. Note that the notation $e^{-j\varphi^{(i)}}$, $i = 1, 2$, stands for the element-wise exponential of the vector $\boldsymbol{\varphi}^{(i)}$.

The assumption in the previous derivation of perfect knowledge of the vector of co-polar symbols $\mathbf{a}_{m\ell}^{(1)}$ at the receiver is not practically feasible. Therefore, as already discussed in [12], this vector can be replaced by a vector of “soft symbols” represented by the *centers of gravity* of the transmitted constellation on the co-polar branch based on the symbol APPs, estimated from bit Log-Likelihood Ratios (LLRs) output by the multi-level decoder. Denoting the vector of centers of gravity as $\boldsymbol{\alpha}_{m\ell}^{(1)}$ and modifying accordingly (9)-(10), the phase estimate for the k -th symbol in the m -th block of the i -th polarization can finally be expressed as

$$\hat{\varphi}_{k,BW}^{(i)} = \arg \left[\Phi_{m\ell}^{(i)} \right] \quad (13)$$

where the subscript BW has been introduced to clearly refer to the BW strategy and

$$\Phi_{m\ell}^{(1)} \triangleq \mathbf{r}_{m\ell}^{(1)} \left(\boldsymbol{\alpha}_{m\ell}^{(1)} \right)^\dagger + \mathbf{r}_{m\ell}^{(2)} \left(\boldsymbol{\alpha}_{m\ell}^{(1)} \right)^\dagger e^{-j\hat{\varphi}_{k,BW}^{(2)}} \quad (14)$$

$$\Phi_{m\ell}^{(2)} \triangleq \mathbf{r}_{m\ell}^{(2)} \left(\boldsymbol{\alpha}_{m\ell}^{(1)} \right)^\dagger e^{-j\hat{\varphi}_{k,BW}^{(1)}} - \mathbf{r}_{m\ell}^{(1)} \left(\boldsymbol{\alpha}_{m\ell}^{(1)} \right)^\dagger. \quad (15)$$

We remark that the notation $\Phi_{m\ell}^{(i)}$ emphasizes that the quantity is computed for the block starting at epoch $m\ell$ using the observable in the i -th polarization.

B. Sliding Window Phase Estimation Strategy

The BW strategy outlined in Subsection III-A can be extended to overcome the limitation of the constant phase assumption at the cost of a higher computational complexity.

input for the IDPE stage at its first iteration. In particular, XPIC is performed to generate the following observable sequence to be input to the demodulator at the first iteration:

$$\tilde{\mathbf{z}}^{(1)}[1] = \left[\mathbf{r}^{(1)} + \mathbf{r}^{(2)} \circ e^{-j\hat{\phi}^{(2)}[0]} \right] \circ e^{-j\hat{\phi}^{(1)}[0]}$$

where $\hat{\phi}^{(1)}[0] = \hat{\phi}^{(2)}[0] = \mathbf{0}$. At the first iteration, the observable sequence thus reduces to $\tilde{\mathbf{z}}[1] \triangleq \mathbf{r}^{(1)} + \mathbf{r}^{(2)}$ and is fed directly to the input of the demodulator, whose soft-outputs are then passed to the soft-input soft-output decoder, which takes into account the presence of multi-level coding. The soft-output decoder generates LLRs on the (multi-level) coded bits, denoted as $\mathbf{L}_{\text{out}}[n]$, where n denotes the iteration number ($n \geq 1$).

In the presence of multi-level coding, the soft-output information associated with the free bits should be computed according to the scheme in Section II. The channel decoder provides soft output information on the coded bits and, therefore, the most likely code sequence can be computed. For $b_1 = 4$, each 4-bit substring identifies a subset of a QAM constellation of size 2^{b-4} , corresponding to $b - 4$ free bits.³ At this point, one can compute the soft output on the free bits based on this subset. The LLRs of the channel coded bits and the free bits can then be combined to generate APPs on the constellation symbols to be used in (14)-(15) or (16). The APPs then feed the phase estimator, which is implemented by the blocks denoted as ‘‘PRE PROC.’’, ‘‘MASTER PHASE EST.’’, and ‘‘SLAVE PHASE EST.’’ already described in Fig. 6. We refer to the combination of a phase estimation act and a demodulation/decoding act as an *external* iteration.

The iterative algorithm can now be summarized as follows. At the n -th iteration, according to XPIC and phase compensation, the phase estimator operates on the following observable vector:

$$\tilde{\mathbf{z}}^{(1)}[n] = \left[\mathbf{r}^{(1)} + \mathbf{r}^{(2)} \circ e^{-j\hat{\phi}^{(2)}[n-1]} \right] \circ e^{-j\hat{\phi}^{(1)}[n-1]}. \quad (17)$$

The vector $\tilde{\mathbf{z}}^{(1)}[n]$ has elements given by (4), where $\hat{\phi}^{(1)}$ and $\hat{\phi}^{(2)}$ at the different iterations can be derived from (5) as detailed in Section III. Phase update recursions can be obtained similarly to the approach shown in [12, eq. (13)]. After a maximum number of external iterations n_{it} , between demapper/decoder and phase estimator, a final decision on the sequence of coded modulated symbols transmitted on the co-polar branch, denoted as $\hat{\mathbf{a}}^{(1)}$, is made.

V. NUMERICAL RESULTS

In this section, we present simulation results for the proposed receiver. The simulation set-up for the considered case study consists of an LDPC-coded M -QAM, where the selected LDPC code is the 7/8-rate code described in [12], with standard belief propagation-based decoding. The parameter χ , defining the XPI intensity, is equal to $\chi = 10^{-\frac{15}{20}}$, i.e., the XPI signal is 15 dB below the co-polar signal. $N_p = 1$ pilot symbol, belonging to a 4-QAM constellation with $E_p = 2.5 E_s$, is inserted in the frame every $N = 50$ symbols. For simulation

³Recall that in all cases we consider $b \geq 4$.

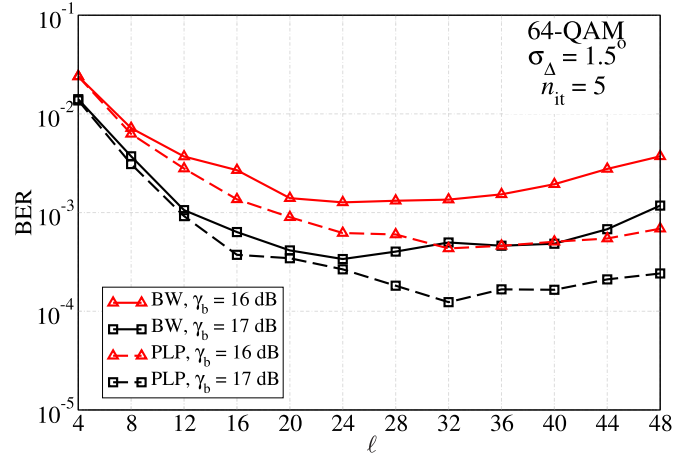


Fig. 9. BER, as a function of ℓ , considering 64-QAM, $n_{\text{it}} = 5$ iterations, $\sigma_{\Delta} = 1.5^{\circ}$, and various γ_b .

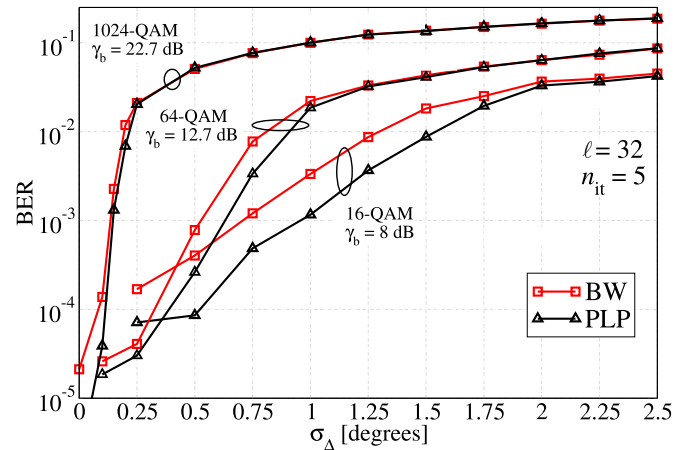


Fig. 10. BER, as a function of σ_{Δ} , considering $n_{\text{it}} = 5$ iterations, $\ell = 32$, and various values of γ_b . The performance of BW and PLP are compared for 16-QAM, 64-QAM, and 1024-QAM.

simplicity, the symbols on the cross-polar branch are generated using the same multi-level coding scheme of the co-polar branch.

In Fig. 9, the BER is shown, as a function of ℓ , considering a scheme with 64-QAM, $n_{\text{it}} = 5$ external iterations, $\sigma_{\Delta} = 1.5^{\circ}$, and various values of γ_b . Both BW and PLP phase estimation strategies are considered.

The value $\ell = 24$ is the best window length for BW (i.e., the value of ℓ which minimizes the BER) for the investigated settings. With the PLP strategy the performance improves, since the lowest achievable BER is less than that of BW and $\ell = 32$ guarantees a good performance in all considered PLP cases. Our results (not shown here for brevity) suggest that $\ell = 32$ is a good compromise value for both BW and PLP and almost all constellation sizes (from 64-QAM to 1024-QAM) and phase noise intensities. Therefore, $\ell = 32$ is adopted in the following results.

In Fig. 10, the BER is shown, as a function of σ_{Δ} , considering schemes with M -QAM (i.e., $M = 16, 64, 1024$), $n_{\text{it}} = 5$ iterations, $\ell = 32$, and various values of γ_b . Both BW and PLP strategies are considered. For each configuration,

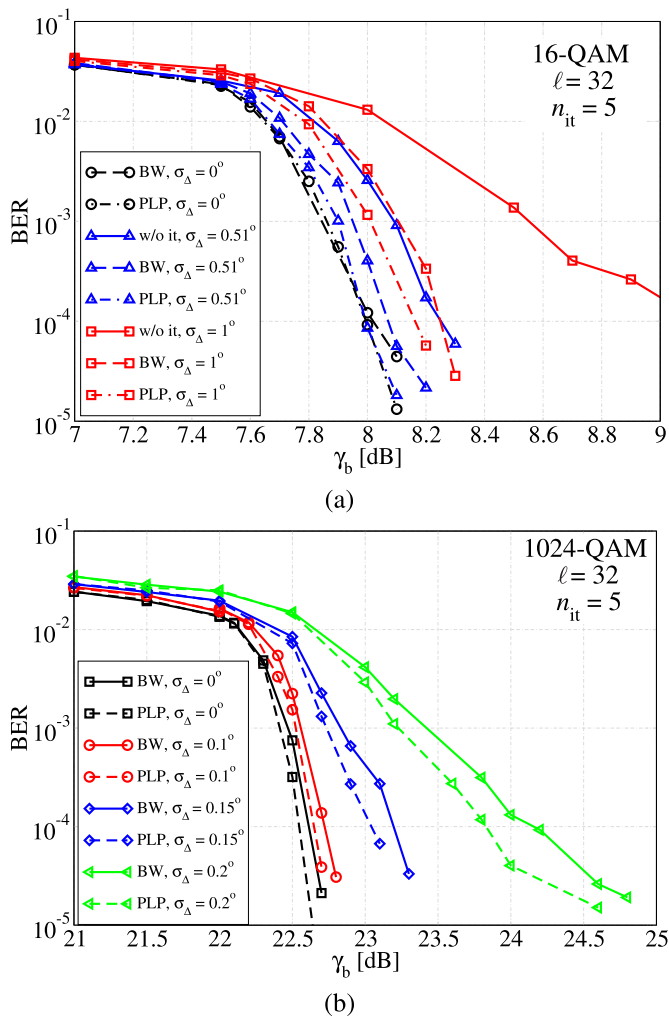


Fig. 11. BER, as a function of γ_b , considering $n_{it} = 5$ iterations, $\ell = 32$, and various values of σ_Δ . The performance of BW and PLP are compared for (a) 16-QAM and (b) 1024-QAM.

it can be observed that PLP outperforms BW for small values of σ_Δ . On the other hand, at high values of σ_Δ the performance of the two approaches is comparable.

Fig. 11, the BER is shown, as a function of γ_b , considering $n_{it} = 5$ iterations, $\ell = 32$, and various values of σ_Δ . The performance of BW and PLP are compared for (a) 16-QAM and (b) 1024-QAM. We remark that multi-level coding is applied to the 1024-QAM case with $b_1 = 4$, so that the constellation is partitioned into 16 subsets with 64 points each. For 16-QAM, we also show the performance of a non-iterative receiver with $n_{it} = 0$, i.e., a system where only rough phase estimation by the CS is performed. For $\sigma_\Delta = 0^\circ$ and $n_{it} = 5$, a reference system, with both CS and IDPE blocks operational and without phase noise, is obtained. The impact of the proposed joint phase estimation and XPIC strategy embedded in the iterative receiver is significant. In fact, the performance drastically improves using the IDPE stage with respect to the non-iterative scenario without this stage operational. Increasing the phase noise intensity degrades the performance and this degradation increases with the constellation size. However, for strong phase noise intensity the performance improvement brought by the

joint PLP phase estimation and XPIC strategy, with respect to the BW strategy, is significant, for both medium- and high-order constellations. Other simulation results (not shown here for conciseness) highlight that further increasing the number of iterations may slightly improve the performance at the cost of higher computational complexity. Finally, note that the values of σ_Δ considered in Fig. 11 are remarkable in comparison with half the minimum angle between two equal-energy constellation points, which is approximately 18.44° for 16-QAM and 1.85° for 1024-QAM constellations.

VI. CONCLUSIONS

This paper presented a solution to the problem of phase synchronization and data detection of independent information streams in DP systems affected by phase noise and XPI. A low-complexity synchronization and decoding iterative receiver was proposed. The APP-based synchronization algorithm performs MMSE-based MS phase estimation with embedded XPIC, whereas the demapping/decoding scheme integrates “off-the-shelf” blocks. The obtained results show very good performance for various constellation sizes, even for challenging phase noise-impaired scenarios.

REFERENCES

- [1] J. Chamberlain, F. Clayton, H. Sari, and P. Vandamme, “Receiver techniques for microwave digital radio,” *IEEE Commun. Mag.*, vol. 24, no. 11, pp. 43–54, Nov. 1986.
- [2] P. Noel and M. Klemes, “Doubling the throughput of a digital microwave radio system by the implementation of a cross-polarization interference cancellation algorithm,” in *Proc. IEEE Radio Wireless Symp.*, Santa Clara, CA, USA, Jan. 2012, pp. 363–366.
- [3] Y. Kurokami, “Cross polarization interference canceller and method of canceling cross polarization interference,” U.S. Patent US 7016438 B2 Mar. 21, 2006.
- [4] G. Milotta and A. Carugati, “Communication between modems in XPIC configuration for wireless applications,” U.S. Patent 8615055 B2, Mar. 30, 2009.
- [5] M. T. Core, “Cross polarization interference cancellation for fiber optic systems,” *J. Lightw. Technol.*, vol. 24, no. 1, pp. 305–312, Jan. 1, 2006.
- [6] E. Ip, A. P. T. Lau, D. J. F. Barros, and J. M. Kahn, “Coherent detection in optical fiber systems,” *Opt. Exp.*, vol. 16, no. 2, pp. 753–791, Jan. 2008.
- [7] K. Roberts, M. O’Sullivan, K. T. Wu, H. Sun, A. Awadalla, D. J. Krause, and C. Laperle, “Performance of dual-polarization QPSK for optical transport systems,” *J. Lightw. Technol.*, vol. 27, no. 16, pp. 3546–3559, Aug. 15, 2009.
- [8] A. Tarable, G. Montorsi, S. Benedetto, and S. Chinnici, “An EM-based phase-noise estimator for MIMO systems,” in *Proc. IEEE Int. Conf. Commun. (ICC)*, Jun. 2013, pp. 3215–3219.
- [9] G. Durisi, A. Tarable, C. Camarda, R. Devassy, and G. Montorsi, “Capacity bounds for MIMO microwave backhaul links affected by phase noise,” *IEEE Trans. Commun.*, vol. 62, no. 3, pp. 920–929, Mar. 2014.
- [10] A. Vizziello, P. Savazzi, and R. Borra, “Joint phase recovery for XPIC system exploiting adaptive Kalman filtering,” *IEEE Commun. Lett.*, vol. 20, no. 5, pp. 922–925, May 2016.
- [11] A. Eliaz, A. Turgeman, A. Aharony, and J. Friedmann, “Modem control using cross-polarization interference estimation,” U.S. Patent 2007/011616, Jul. 10, 2008.
- [12] M. Martalò *et al.*, “Pragmatic phase noise compensation for high-order coded modulations,” *IET Commun.*, vol. 10, no. 15, pp. 1956–1963, Oct. 2016.
- [13] M. Martalò *et al.*, “Phase noise compensation for dually-polarized systems with independent transmission streams,” in *Proc. IEEE Int. Symp. Wireless Commun. Syst. (ISWCS)*, Brussels, Belgium, Aug. 2015, pp. 251–255.

- [14] A. Demir, A. Mehrotra, and J. Roychowdhury, "Phase noise in oscillators: A unifying theory and numerical methods for characterization," *IEEE Trans. Circuits Syst. I, Fundam. Theory Appl.*, vol. 47, no. 5, pp. 655–674, May 2000.
- [15] J. Rutman and F. L. Walls, "Characterization of frequency stability in precision frequency sources," *Proc. IEEE*, vol. 79, no. 7, pp. 952–960, Jul. 1991.
- [16] J. K. Cavers, "An analysis of pilot symbol assisted modulation for Rayleigh fading channels," *IEEE Trans. Veh. Technol.*, vol. 40, no. 4, pp. 686–693, Nov. 1991.
- [17] G. Ferrari, G. Colavolpe, and R. Raheli, "On linear predictive detection for communications with phase noise and frequency offset," *IEEE Trans. Veh. Technol.*, vol. 56, no. 4, pp. 2073–2085, Jul. 2007.
- [18] J. M. Torrance and L. Hanzo, "Comparative study of pilot symbol assisted modem schemes," in *Proc. Int. Conf. Radio Receivers Assoc. Syst.*, Bath, U.K., Sep. 1995, pp. 36–41.



algorithms for wireless systems and networks. He was a co-recipient of a best student paper award at IWWAN 2006, and also won, as part of the WASNLab Team, the First Prize Award at the 2011 BSN Contest.

Marco Martalò (SM'16) received the Ph.D. degree in information technologies from the University of Parma, Italy, in 2009. He was a Visiting Scholar with EPFL, Switzerland, from 2007 to 2008. Since 2012, he has been an Assistant Professor with E-Campus University, Italy, and also a Research Associate with the University of Parma, Italy. He has co-authored the book *Sensor Networks with IEEE 802.15.4 Systems: Distributed Processing, MAC, and Connectivity*. His research interests are in the design of communication, and signal processing



processing, advanced communication and networking, and IoT and smart systems. He has authored extensively in these areas.

Gianluigi Ferrari (SM'12) received the Laurea (*summa cum laude*) and Ph.D. degrees in electrical engineering from the University of Parma, Parma, Italy, in 1998 and 2002, respectively. Since 2002, he has been with the University of Parma, where he is currently an Associate Professor of Telecommunications (with National Scientific Qualification for Full Professorship since 2013), and also is currently the Coordinator of the Internet of Things (IoT) Laboratory, Department of Engineering and Architecture. His research interests include signal



reconfigurable architectures.

Muhammad Asim received the B.S. degree in electrical engineering from Cocos University, Pakistan, in 2009, the M.Eng. degree in information and communication from Chosun University, South Korea, in 2012, under the NIPA Scholarship Program, and the Ph.D. degree in information technologies from the University of Parma, Italy, in 2016. He is currently with the Department of Computer Science, Preston University, Pakistan. His research interest includes channel coding schemes, softdecision directed iterative receivers in fading channels, and



aspects of wireless communications and statistical signal processing.

Jonathan Gambini received the M.Sc. (*summa cum laude*) and Ph.D. degrees in telecommunications engineering from the Politecnico di Milano, Italy, in 2007 and 2010, respectively. In 2007, he was a Visiting Researcher with CWCSR, New Jersey Institute of Technology, NJ, USA. In 2011, he was a Research Associate with the Dipartimento di Elettronica e Informazione, Politecnico di Milano, with a focus on distributed antennas systems. Since 2012, he has been with Huawei Technologies. His research interests concern algorithmic and information-theoretic



high-power amplifiers digital predistortion, phase noise suppression, and MIMO for point-to-point microwave links. He is currently involved in researching phased array processing and the development of mmWave 5G BTS systems.

Christian Mazzucco received the Laurea degree in telecommunications engineering from the University of Padova, Italy, in 2003, and the master's degree in information technology from the Politecnico di Milano in 2004. In 2004, he joined Nokia Siemens Networks, Milan, where he was involved in research on UWB localization and tracking techniques. From 2005 to 2009, he was involved in several projects mainly researching and developing Wimax systems and high-speed LDPC decoders. In 2009, he joined Huawei Technologies, Italy, studying algorithms for



Technologies. He has worked on LDPC convolutional codes, with two patents on parity-check matrix constructions, and estimation algorithms for MIMO systems. He has co-authored several patents and papers in international journals and conferences.

Giacomo Cannalire received the Laurea degree in electronic engineering from the Politecnico di Torino in 1980. From 1981 to 2009, he was with the Switching, Radiomobile, and Microwave Divisions, Nokia Siemens Networks (GTE, Italtel, Siemens). He has carried out, using digital signal processors, channel associated signaling (No.5, R1, R2), echo cancelers for international telephone connections, speech transcoding devices for GSM networks, and LDPC block codes for channel coding. Since 2010, he has been with the Milan Research Center, Huawei



equalization, synchronization, digital predistortion, and MIMO processing.

Sergio Bianchi received the Laurea degree in electronic engineering from Pavia University in 1983. In 1984, he joined GTE and was involved in research and developing projects of microwave digital radio links. He is currently with the Milan Research Center, Huawei Technologies. He has authored papers in international journals and conferences and has patents on digital signal processing and microwave communications. His research interests include algorithms applied to microwave communications, modulation-demodulation, channel coding,



proceedings, scientific monographs and industrial patents. He has served as an Editorial Board Member and the Technical Program Committee Co-Chair of prestigious international journals and conferences.

Riccardo Raheli (M'87) has been a Professor of Communication Engineering at the University of Parma, Italy, since 1991. Previously, he was with the Scuola Superiore S. Anna, Pisa, from 1988 to 1991, and Siemens Telecomunicazioni, Milan, from 1986 to 1988. In 1990 and 1993, he was a Visiting Assistant Professor at the University of Southern California, Los Angeles, USA. His scientific interests are in the general area of information and communication technology, in which he has authored extensively in quality journals, conference